

Runoff Estimation for the Central Region of the Lesser Zab River Watershed Using the SCS-Curve Number Method and GIS

Qasim Mohammed Khudair Salman^{1*}, Ahmed Naseh Ahmed Hamdan¹

¹ Department of Civil Engineering, Engineering College, University of Basrah, Basrah, Iraq

* Corresponding author's e-mail: qasim2alali@gmail.com

ABSTRACT

This study aimed to develop a hydrologic model for the central region (central catchments) located between Doka and Al-Dibis dams in the Lesser Zab River (LZR) watershed, in Iraq. The hydrologic structure of the study area was prepared based on the DEM layer with 12.5 m spatial resolution by using the GIS environment, and then the HEC-HMS software was used for simulating the main hydrological processes like the infiltration losses, transformation, channel routing, and the baseflow contribution by using the SCS-CN, SCS-UH, Muskingum, and the Recession methods respectively. The corrections of the CN parameter due to the effects of the slope and initial abstraction were used and the resulting CN values for the entire LZR watershed were ranging from 56 to 100. This study concluded the effectivity of using the GIS environment and HEC-HMS software in the continuous rainfall-runoff modelling and achieved very good performance with R^2 and NSE criteria of 0.9115 and 0.9 under the calibration phase, while 0.925 and 0.91 values were achieved for the same criteria under the validation phase respectively, also the CN was the most sensitive parameter in the proposed hydrologic model.

Keywords: Digital Elevation Model (DEM), Lesser Zab River (LZR) watershed, Rainfall-Runoff modelling, SCS-CN method, GIS, HEC-HMS.

INTRODUCTION

Water resources management is considered essential for the right control of the water resources in a sustainable manner at the basin scale. In Iraq, the increase in water demand due to the high population rate, bad strategies for water preservation, and the effect of dams outside of Iraq applied huge stress on the limited water resources inside Iraq causing a water shortage [Al-Ansari and Knutsson, 2011; Salman and Hamdan, 2022]. The runoff, which is considered one of the most dangerous parameters of the hydrologic cycle on the human life, needs to be prevented from flooding and stored for various usage, thus the runoff estimation is considered very important for the right management of the basin [Al-Ansari and Knutsson, 2011].

The United States Army Corps of Engineers (USACE) developed a special software with integrated tools called the Hydrologic Engineering

Center-Hydrological Modeling System (HEC-HMS) to construct dendritic models for the basins and estimate the runoff volume mainly. The HEC-HMS software can simulate all the hydrological processes in the basin like the rainfall losses, base flow, and routing using various methods, one of these methods is the Soil Conservation Services-Curve Number (SCS-CN) method for estimation of the rainfall losses and runoff volume in term of the fallen rainfall [Halwatura and Najim, 2013]. The SCS-CN method comprises all the influent parameters on the runoff generation like the soil types and the Land Use/ Land Cover (LULC) into one parameter called the CN parameter, hence the SCS-CN method is considered reasonably simple, and widely accepted method for estimating the runoff [Klari and Ibrahim, 2021].

Several researchers used the SCS-CN method, GIS, and the HEC-HMS for the rainfall-runoff modelling successively. In this regard Oleyiblo and Li [2010] studied the applicability

of using the HEC-HMS software for flood forecasting in the Misai and Wan'an watersheds in China, the HEC-HMS model was calibrated and validated with recorded flood events reaching a very good efficiency of the proposed model. Gurm and Tolessa [2014] estimated the runoff volume for the Tandava River Basin in India by using the remotely sensed data (RS) and the GIS environment for the processing, they succeeded in the estimation of the runoff based on the SCS-CN method indicating the effectivity of this method and the GIS for the runoff estimation. Kaffas and Hrisanthou [2014] studied the applicability of performing a continuous hydrological model using the HEC-HMS for the Kosynthos River basin in Greece by applying the SCS-CN method, they achieved a successful model with Nash Sutcliffe Efficiency (NSE) equal to 0.84 and R^2 equal to 0.86, they concluded that the SCS-CN method could be used for the continuous modelling effectively. Tassew et al. [2019] made a hydrological model to simulate the rainfall-runoff on the Gilgel Abay catchment in Ethiopia by using the HEC-HMS with the SCS-CN method for the runoff estimation, their model succeeded in the calibration and achieved very good efficiency in the validation with 0.884 for the NSE and 0.925 for the R^2 , also they concluded that the CN was the most sensitive parameter in the model. Dinka and Klik [2020] achieved the same trend of results and conclusions by Tassew et al. [2019], but also concluded that the LULC changes of the Basaka catchment in Ethiopia, where the study was achieved, have the biggest effect on the CN values and the runoff generation. Pokhrel and Karki [2021] studied the suitability of using the SCS-CN method to estimate the runoff of the Tamor River basin in Nepal using HEC-HMS, the model was calibrated and validated successfully with NSE equal to 0.8 and R^2 equal to 0.82 indicating the high performance of the model. Jabbar et al. [2021] estimated the direct runoff of the Putrajaya catchment in Malaysia by using the SCS-CN method within the HEC-HMS, the performance of the model was very good with NSE equal to 0.92 and R^2 equal to 0.9 indicating the model perfection. Hamdan et al. [2021] made a hydrological model of Al-Adhaim River catchment in the northeast of Iraq using the HEC-HMS software and based on the SCS-CN method to estimate the runoff volume, they concluded that the SCS-CN based model was very effective with R^2 equal to 0.9, also they concluded that the CN and the

initial abstraction (Ia) were the most sensitive parameters in the model. Alrammahi and Hamdan [2022] made a hydrological model of the Diyala River catchment in Iraq using the HEC-HMS and GIS software, they were doing a sensitivity analysis as well as a calibration and verification for the model through the period of 2017–2021, they get an accuracy of the results of about 95%.

Due to the limited hydrological studies of the watersheds in Iraq, this study aimed to develop a validated HEC-HMS model for the Lesser Zab River (LZR) watershed in Iraq, specifically for the central catchments (central region) located between Dokan and Al-Dibis dams, only these catchments were selected because of the absence of recorded flow data for the remain catchments in the watershed.

METHODOLOGY

This section describes the study area, the procedure for data processing using the GIS environment, hydrological processes for the model in the HEC-HMS and the influent parameters for these processes, trusted sources for the main Remote Sensing (RS) data layers used in this study like the DEM layer, soil data layer, and the LULC layer, parameters estimation, climatological data, and the performance indices used for judging the model efficiency.

Study area

The Lesser Zab River (LZR) or Lower Zab River, see Figure 1, is one of the main five tributaries of the Tigris River in the northern region of Iraq, other tributaries are the Upper Zab River, Al-Khabour River, Al-Adhaim River, and Sirwan (Diyala) River [Saeedraashed and Guven, 2013]. Administratively, the LZR watershed is located within the boundaries of the following Iraqi governorates; Erbil, Al-Sulaymaniyah, and Kirkuk, representing 76% of the gross watershed area, while the remaining 24% of the area including the origin of the river is located in Iran [UN-ESCWA, 2013]. In Iraq, the Tigris River runs south of Al-Sharkat city and meets the LZR near Al-Zuwiya village, about 30 km north of Al-Fatha city and 220 km north of Baghdad [UN-ESCWA, 2013]. The LZR watershed has an elevation range from 128 to 3619 MASL, a total area of about 19780 km², and a river length

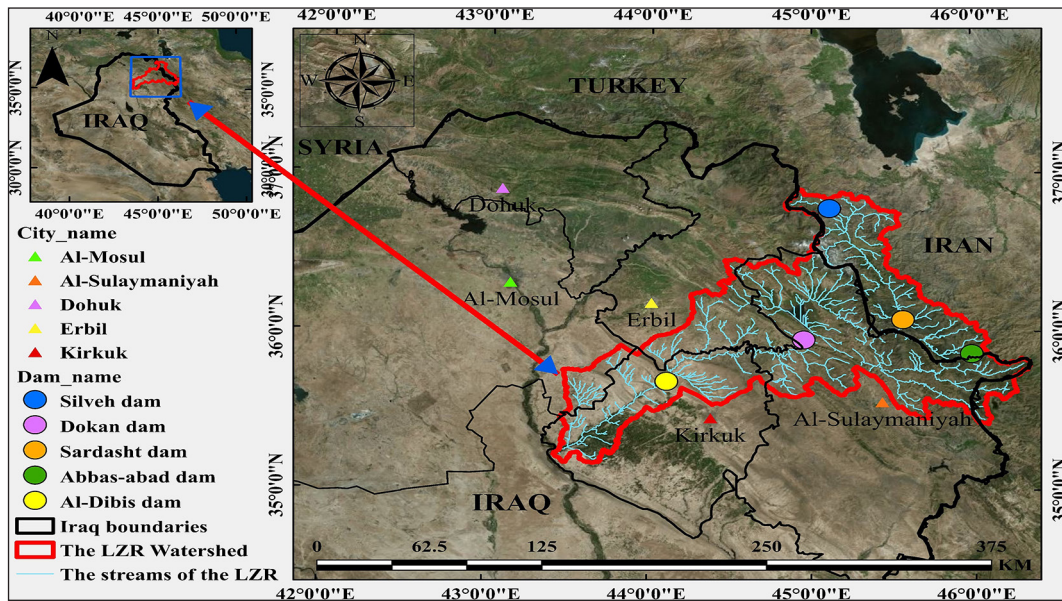


Figure 1. Location of the LZR watershed in the local region

of about 456 km [UN-ESCWA, 2013]. The LZR watershed is located approximately from WE longitude of 43.39° to 46.26° and from SN latitude of 35.16° to 36.79° [Saeedrashad and Guven, 2013]. Generally, the Tigris River is mainly fed by the precipitation and the snow melting in the headwater region [Noori et al, 2019], the rainfall season usually starts from October till the end of April or sometimes to the mid of May [Hamdan et al., 2021], therefore, the peak flow of the LZR usually occurred in the spring season, specifically in April month because of the heavy rainfall and the gradual snow melting in the headwater region, while the minimum flow occurs in September [UN-ESCWA, 2013]. The

LZR watershed includes many influent dams like Dokan and Al-Dibis dams in Iraq, as well as Sardasht Dam in Iran near the Iraqi-Iranian boundaries [Salman and Hamdan, 2022; UN-ESCWA, 2013].

In general, Dokan Dam is an arched concrete dam located about 65-67 km to the north-west of Al-Sulaymaniyah city, 295 km to the north of Baghdad with an exact location of 35° 57' 15" N and 44° 57' 10" E near to the Ranya city, on the other hand, Al-Dibis Dam is located on the LZR in Kirkuk governorate with about 130 km upstream of the confluence of the LZR with the Tigris River and 60 km to the north-west of Kirkuk city with an exact location of 35° 41' 25"

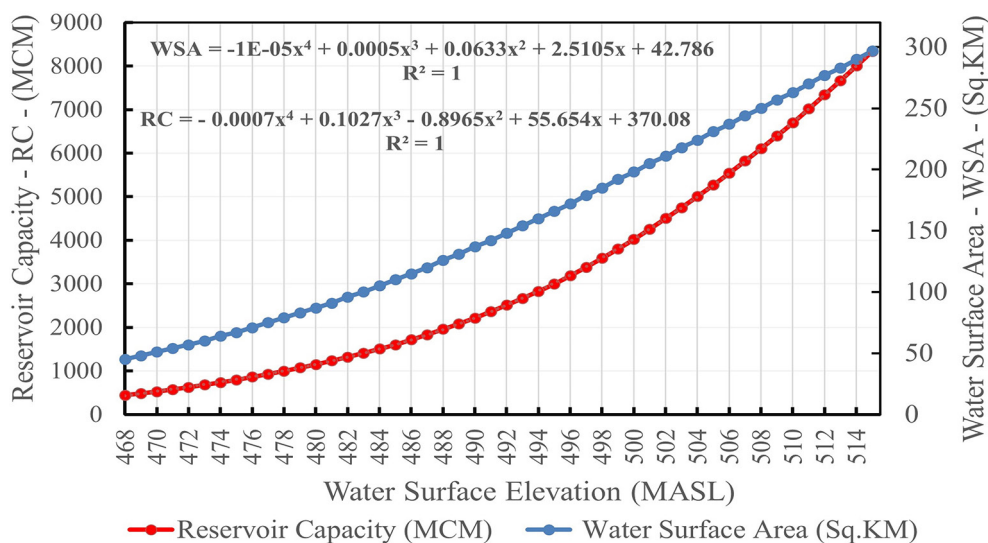


Figure 2. Paired characteristics of Dokan reservoir (elevation-area-storage capacity)

N and 44° 6' 34" E [Al-Ansari et al, 2018]. The important paired characteristics of Dokan reservoir that are needed by the HEC-HMS software for the right modelling are illustrated in Figure 2, these data were obtained from the Ministry of Water Resources in Iraq (MOWR).

Data processing

To develop the hydrologic structure of the LZR watershed, the Digital Elevation Model (DEM) layer with a high spatial resolution of 12.5 m was downloaded from the Alaska Satellite Facility (ASF) of the National Aeronautics and Space Administration (NASA) [NASA Earth Data, <https://search.asf.alaska.edu> (accessed on 20 February 2023)] as Raw DEM layer, then the HEC-GeoHMS extension was used to get the basic hydrological layers, create the subbasins and rivers in the watershed, extract the hydrologic characteristics, estimate the parameters, and create the hydrologic structure of the LZR watershed, see Figure 3.

Adopted hydrologic processes and parameters estimation

This study implemented the SCS-CN method for simulating the losses, whereas the SCS-UH, Muskingum, and Recession methods were chosen for the simulation of the transformation,

channel routing, and the baseflow contribution respectively. The canopy interception, surface depression storage, and evapotranspiration in terms of the temperature degrees also were used in this study. The mechanism of estimating the main parameters is explained in the following sections.

Soil conservation service-curve number (SCS-CN) method for the losses

The Soil Conservative Service-Curve Number (SCS-CN) is one of the famous and important methods suggested by the USDA used for estimating the infiltration losses in the watershed, nowadays the SCS-CN method becomes a very accepted technique because of its ability to comprise all the influent variables that affect the runoff generation like the soil types or Hydrological Soil Groups (HSGs), LULC categories, and the Antecedent Moisture Conditions (AMCs) into one required parameter called the (CN) parameter to estimate the direct runoff [Klari and Ibrahim, 2021]. This study adopted the average condition of the AMCs; thus, the soil types and LULC layers were only the influent variables on the CN parameter. Eq. 1 represents the standard SCS-CN equation, but this study adopted some corrections on the CN parameter due to the initial abstraction (Ia) and the slope effects as illustrated next.

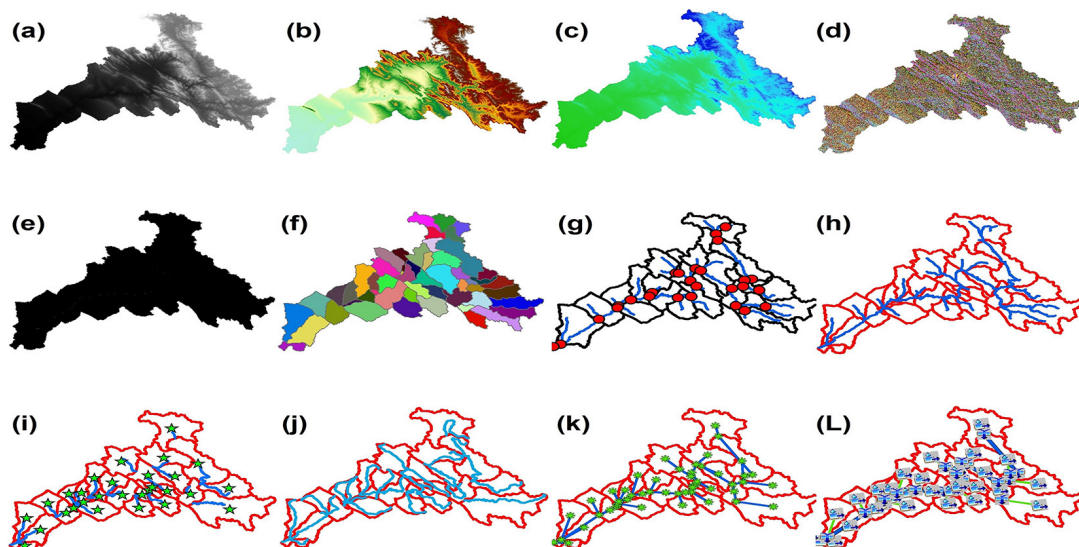


Figure 3. The basic layers of the LZR watershed using the HEC-GeoHMS extension inside the GIS environment, (a) Clipped Raw DEM, (b) DEM reconditioning, (c) fill sink, (d) flow direction, (e) flow accumulation, (f) catchments raster, (g) adjoint catchments, (h) subbasins and rivers across the watershed, (i) centroids of the subbasins and the centroidal longest flow paths, (j) longest flow path, (k) HEC-HMS schematic, and (l) the final hydrologic structure of the LZR watershed illustrated with the HEC-HMS legend

$$Q = \frac{(P - Ia)^2}{P - Ia + S} = \frac{(P - 0.2S)^2}{P + 0.8S} \text{ only for } p > 0.2S \quad (1)$$

$$S = \frac{25400}{CN} - 254 \quad (2)$$

where: Q – the direct surface runoff depth (mm);
 P – the total precipitation (mm);
 Ia – initial abstraction (mm);
 S – the maximum potential infiltration or abstraction (mm).

Many researchers adopted the ratio of the initial abstraction to be equal to 0.05 instead of 0.2 and obtained better results in their models depending on Eq. 3, and 4 [Klari and Ibrahim, 2021].

$$S_{0.05} = 1.33 * S_{0.2}^{1.15} \quad (3)$$

$$Q = \frac{(P - 0.05S_{0.05})^2}{P + 0.95S_{0.05}} \text{ only for } p > 0.05S \quad (4)$$

where: $S_{0.2, 0.05}$ – represent the maximum potential abstraction (inch) for the ratio (λ) of 0.2 and 0.05 respectively.

Generally, the CN is a dimensionless parameter ranging from 0 to 100, the lowest value is referred to as the lowest potential runoff, while the highest value is referred to as the highest potential runoff. The basic source for the CN values under all conditions of the HSGs, LULC, and AMCs is the Technical Release (TR-55) from the USDA but only for a 5% slope of the catchments and ratio (λ) of 0.2 [Cronshey, 1986], the increase in the average slope percentage of the basin basically reduce the infiltration time and consequently increase the runoff volume, thus, this study adopted the modified equation of Sharpley and Williams, which is Eq. 5, and Huang equation, which is Eq. 7, for the right CN values estimation under the effect of the slope [Huang et al., 2006].

$$CN_{II-\alpha} = 0.8794(CN_{III} - CN_{II}) * (1 - 1.0311e^{-0.6116\alpha}) + CN_{II} \quad (5)$$

$$CN_{III} = \frac{CN_{II}}{0.427 + (0.00573 * CN_{II})} \quad (6)$$

$$CN_{II-\alpha} = CN_{II} * \frac{322.79 + 15.63 \alpha}{323.52 + \alpha} \quad (7)$$

where: CN_{II} – the CN parameter under the average condition of AMCs (directly called the CN);
 CN_{III} – the CN parameter under the wet condition of AMCs;
 $CN_{II-\alpha}$ – the corrected CN_{II} for the slope effect;
 α – represents the slope of the catchment (m/m).

Due to Huang et al. [2006], if the variable (α) was in the range of (0.14–1.4) for the catchment, then Eq. 7 will be used, otherwise, Eq. 5 will be used.

In the end, the SCS-CN method is preferred over the other methods for losses estimation because it is considered a simple method that relies on one parameter, easy method to understand, predictable method, has a stable conceptual technique, and supported method by well-documented inputs and empirical data, in other words, it is considered well established, wide applicable, and accepted globally [Subramanya, 2008].

To generate the CN map of the LZR watershed, the soil data and LULC layers must be prepared and merged by the HEC-GeoHMS extension, these layers are described next:

- a) soil types and hydrological soil groups (HSGs) – the soil components are classified as silt, clay, sand, and gravel based on the grain size, depending on these components, the soil texture and the HSGs could be defined. The USDA-SCS classified the soil hydrologically into four groups which are A, B, C, and D according to the minimum infiltration rate for each texture class [Subramanya, 2008], each one of the previous soil groups has its own range of the CN parameter. The soil data of the LZR watershed including the soil texture and the corresponding HSGs were prepared depending on the soil portal of Food and Agricultural Organization (FAO) [FAO, <https://www.fao.org/soils-portal/HWSD> (accessed on 5 March 2023)]. As illustrated in Figure 4, the dominant topsoil of the LZR watershed is loamy soil with 86% of the watershed area, while the remaining 14% is clayey soil.
- b) land use/land cover (LULC) layer – the land use/land cover (LULC) layer describes the nature of the earth’s surface and the type of

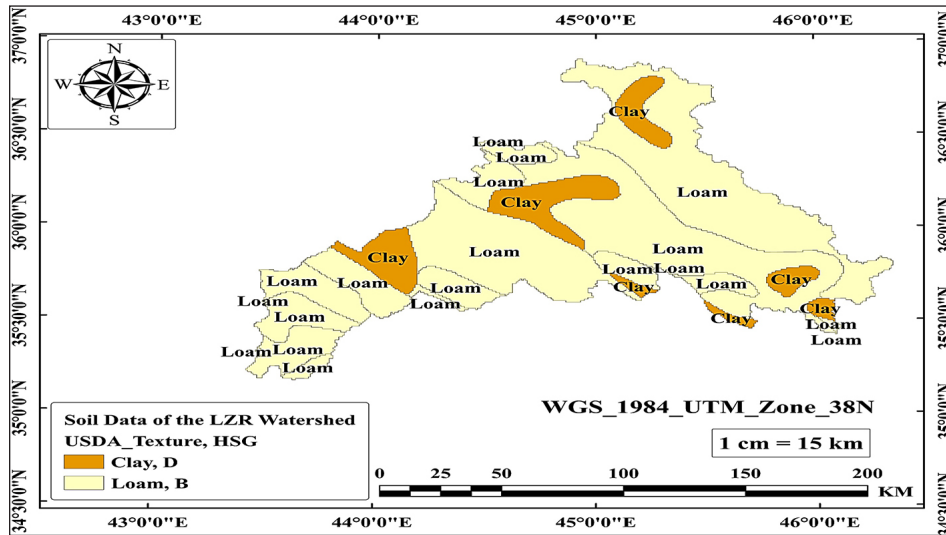


Figure 4. Top soil texture and the corresponding HSGs of the LZR watershed

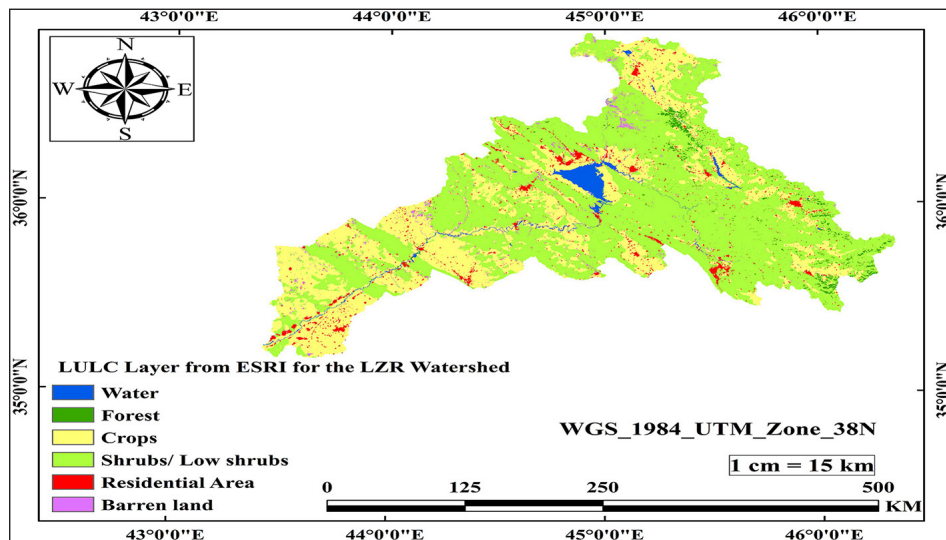


Figure 5. LULC layer of the LZR watershed

land utilization [Cronshey, 1986]. The LULC has the main influence on the CN value according to the continuous temporal changes of the LULC classes and their effects on the watershed infiltration [Khzr et al., 2022]. The LULC layer for this study was obtained from the Environmental Systems Research Institute (ESRI) with 10 m spatial resolution [ESRI, <https://www.arcgis.com/LULC> (accessed on 10 March 2023)]. As illustrated in Figure 5, the largest class of the LULC layer with about 65% of the LZR watershed area involves a mix of shrubs, scattered low shrubs, savanna, and single bushes. The second major class is the crops land with about 25% of the watershed area and mostly planted with wheat and barley.

Soil conservation service-unit hydrograph (SCS-UH) for the transformation

The SCS proposed a curvilinear Unit Hydrograph (UH) model for the transformation process and converting the excess rainfall to a runoff volume, the main hypothesis of the (UH) derivation is that the excess rainfall and resulting runoff are directly related to each other [Subramanya, 2008]. The only required input for the SCS-UH method is the lag time, which is defined as the time between the centroid of precipitation mass and the peak point of the runoff hydrograph, the lag time could be calculated based on Eq (8) automatically by the HEC-GeoHMS extension.

$$Lag\ Time(min) = \frac{60[L^{0.8}(S + 1)^{0.7}]}{1900Y^{0.5}} \quad (8)$$

$$S = \left[\frac{1000}{CN} - 1 \right] \tag{9}$$

where: *L* – longest flow path (feet);
Y – average basin slope (%);
S – maximum potential retention (inches).

Canopy storage and surface depressions storage

The canopy interception is one of the important storage components in the subbasins element, especially for the continuous modelling, the canopy storage is represented by the amount of precipitation that has been captured by the trees, shrubs, and grasses. The canopy maximum storage is a function of the vegetation type, see Table 1. The surface storage is the volume of precipitation that is not captured by the canopy and falls directly to the land surface to be stored in the small surface depressions, the depression maximum storage is a function of the catchment slope, see Table 2.

Muskingum and recession methods for the channel routing and baseflow contribution

In general, flood routing is a method of predicting the flood hydrograph shape in the river channel by taking into account all the influent factors like the channel storage, and resistance

characteristics of the river. The Muskingum method is one of the most common methods for the flood routing, this method estimates the detention and attenuation of the downstream hydrograph by introducing only two parameters, which are the wave travel time (*K*) and weighting factor (*X*) [Subramanya, 2008]. The Recession method is used to simulate the interflow and baseflow contribution to the downstream hydrograph by introducing only three parameters, which are the initial discharge, recession constant, and the baseflow threshold point in the hydrograph.

All the previous parameters for the routing and baseflow contribution processes were set up initially in the HEC-HMS model and the correct values for these parameters will be concluded only by the calibration and validation processes of the HEC-HMS model.

Climatological data

In this study, all the climatological data, especially the rainfall data were obtained from the NASA climatological database [POWER, Data Access Viewer, <https://power.larc.nasa.gov> (accessed on 15 March 2023)] to accomplish the continuous rainfall-runoff simulation during the calibration period of 2014–2016, and the validation period of 2017–2019. See Figure 6 for the daily rainfall over the central catchments (with the prefix of *W*) of the LZR watershed.

Table 1. Values of the maximum canopy storage [Ahbari et al., 2018]

Types of vegetation	Max storage (mm)	Land use/land cover classes
Vegetation is not directly known	1.270	Small grain, straight row, good condition
Grasses and deciduous trees	2.032	Brush + pasture, with all in fair condition
Coniferous trees	2.540	Pinyon, good+ fair + bad condition

Table 2. Values of the maximum surface storage [Ahbari et al., 2018]

Land surface description	Slope (%)	Max surface storage (mm)
Paved impervious area	NA	3.2–6.4
Steep, smooth slopes	>30	1
Moderate to gentle slope	5–30	12.7–6.4
Flat, Furrowed land	0–5	50.8

Table 3. Rating of the performance criteria for watershed-scale models [Ouédraogo et al., 2018]

Performance criteria	Very good	Good	Satisfactory	Unsatisfactory
<i>R</i> ²	>0.75–1	0.65–0.75	0.5–0.65	≤0.5
NSE	>0.75–1	0.65–0.75	0.5–0.65	≤0.5
PBIAS %	<±10	±10–±15	±15–±25	≥±25

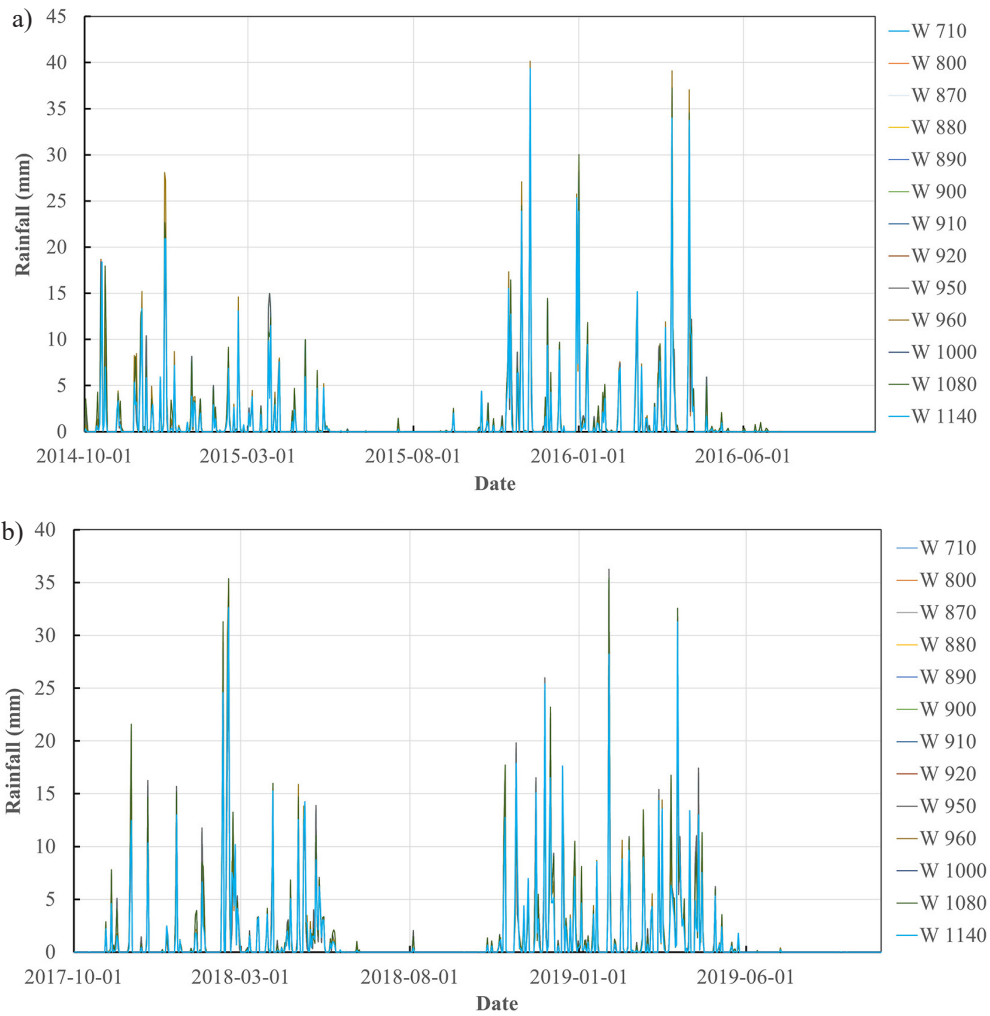


Figure 6. Daily precipitations, (a) for 2014–2016, and (b) for 2017–2019

Performance indices

The performance criteria used for this study were the coefficient of correlation (R^2), Nash-Sutcliffe model Efficiency (NSE), and the

Percent BIAS (PBIAS). These adopted criteria were calculated automatically by the HEC-HMS software for every simulation run, the categorization limits of these criteria are illustrated in Table 3.

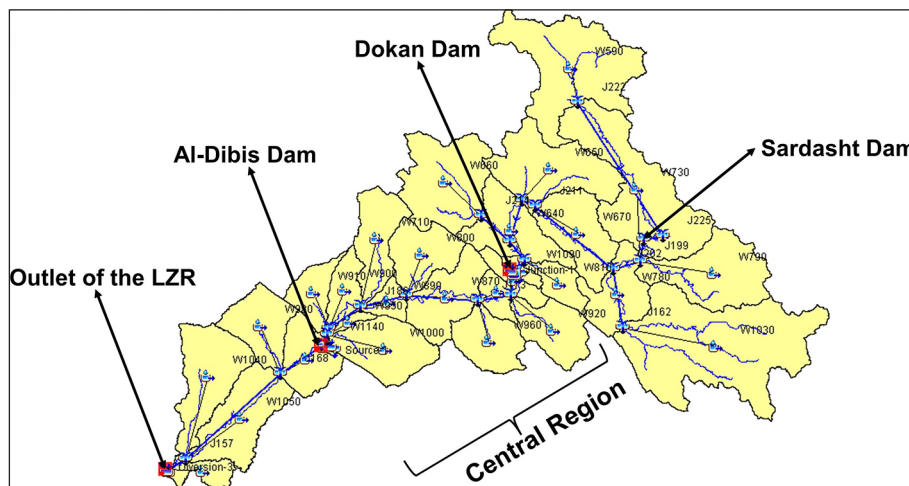


Figure 7. The LZR watershed model in the HEC-HMS Software

RESULTS

The hydrologic model of the LZR watershed was exported from the HEC-GeoHMS extension to the HEC-HMS software to set up all the required inputs for the basin model, metrological model, control specification, time series data manager, and the paired data manager for the existing reservoirs, see Figure 7 for the LZR watershed model in the HEC-HMS. The first simulation runs for the catchments located in the central region have low values of the performance criteria, hence the calibration and validation processes were mostly done.

Curve number (CN) map of the LZR watershed

The resulting CN map of the LZR watershed was achieved by merging the attributes of the soil and LULC layers using the HEC-GeoHMS extension, see Figure 8. This layer is very important for the CN and lag time average values estimation for each catchment.

Calibration process

In this study, the calibration process was done for the water years of 2014–2015 and 2015–2016. In Iraq, the water year starts on 1st October and ends on 30th September for the next year. In this

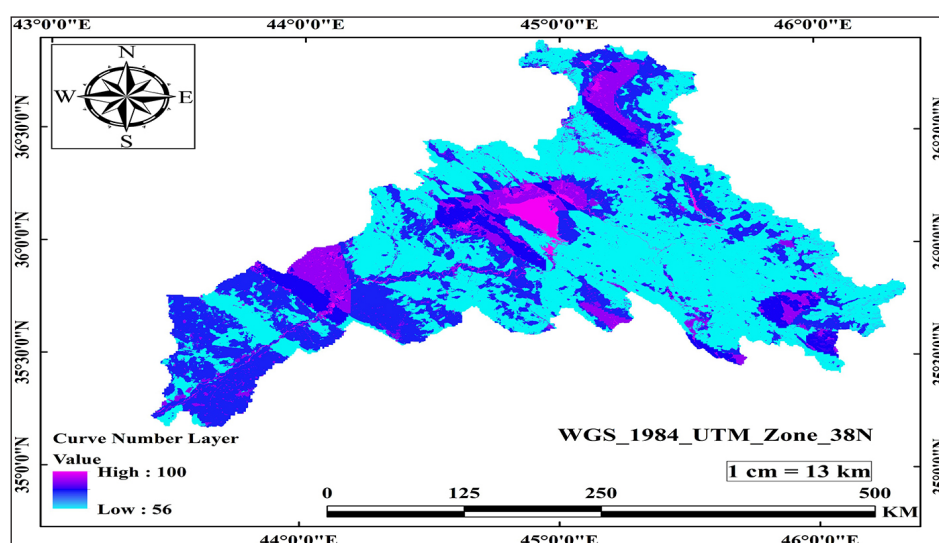


Figure 8. Curve number (CN) map of the LZR watershed

Table 4. Optimized parameters of the central catchments in the LZR watershed

Catchment name	SCS-CN method parameters			Lag time (min)	Max. canopy storage (mm)	Max. surface depression storage (mm)
	Initial $CN_{0.05\alpha}$	Optimized $CN_{0.05\alpha}$	Impervious area %			
W 710	71.708	70.099	1.031	431.59	0.235	16.673
W 800	75.641	73.944	3.864	284.64	0.337	19.909
W 870	74.091	72.429	2.002	429.35	0.256	18.564
W 880	75.771	74.071	1.328	215.34	0.651	20.377
W 890	72.854	71.219	0.917	257	0.364	22.041
W 900	76.290	74.579	1.792	333.03	0.499	26.328
W 910	87.168	85.212	2.894	442.87	0.831	40.526
W 920	63.916	62.482	5.085	324.49	1.812	17.596
W 950	73.996	72.336	4.382	266.54	1.280	35.964
W 960	68.072	66.544	1.752	303.97	0.450	18.899
W 1000	71.273	69.674	3.397	488.73	0.851	31.381
W 1080	53.543	52.342	5.097	189.16	2.274	9.792
W 1140	90.683	88.648	1.334	75.086	0.084	24.805

Note: the $CN_{0.05\alpha}$ – the CN parameter corrected to the (Ia) and the slope effects.

study, the outflow discharge data from Dokan Dam were interred into the model as a boundary condition, while the inflow discharge data to Al-Dibis reservoir was used to judge the general efficiency of the central region model. The optimized parameters for the central catchments are illustrated in Table 4.

The optimized ranges for the parameters of Muskingum and Recession methods for all the central catchments were (3.1–3.8) hours for the travel time K, (0.14–0.18) for the weighting factor X, (1.84–1.97) m³/sec for the baseflow initial discharge, (0.78–0.89) for the recession constant, and (0.08–0.12) for the ratio-to-peak parameter.

The initial and optimized values of the corrected CN in Table 4 were close to each other, which indicates the perfect procedure used to estimate the initial values of the CN parameter and the accurate used layers in this study. Low values of the parameters that belong to the recession method could indicate

Table 5. Performance criteria of the central region model under the calibration phase

Water year	R ²	NSE	PBIAS %
2014–2015	0.884	0.866	5.38
2015–2016	0.939	0.935	3.33
Average	0.9115	0.9	4.355

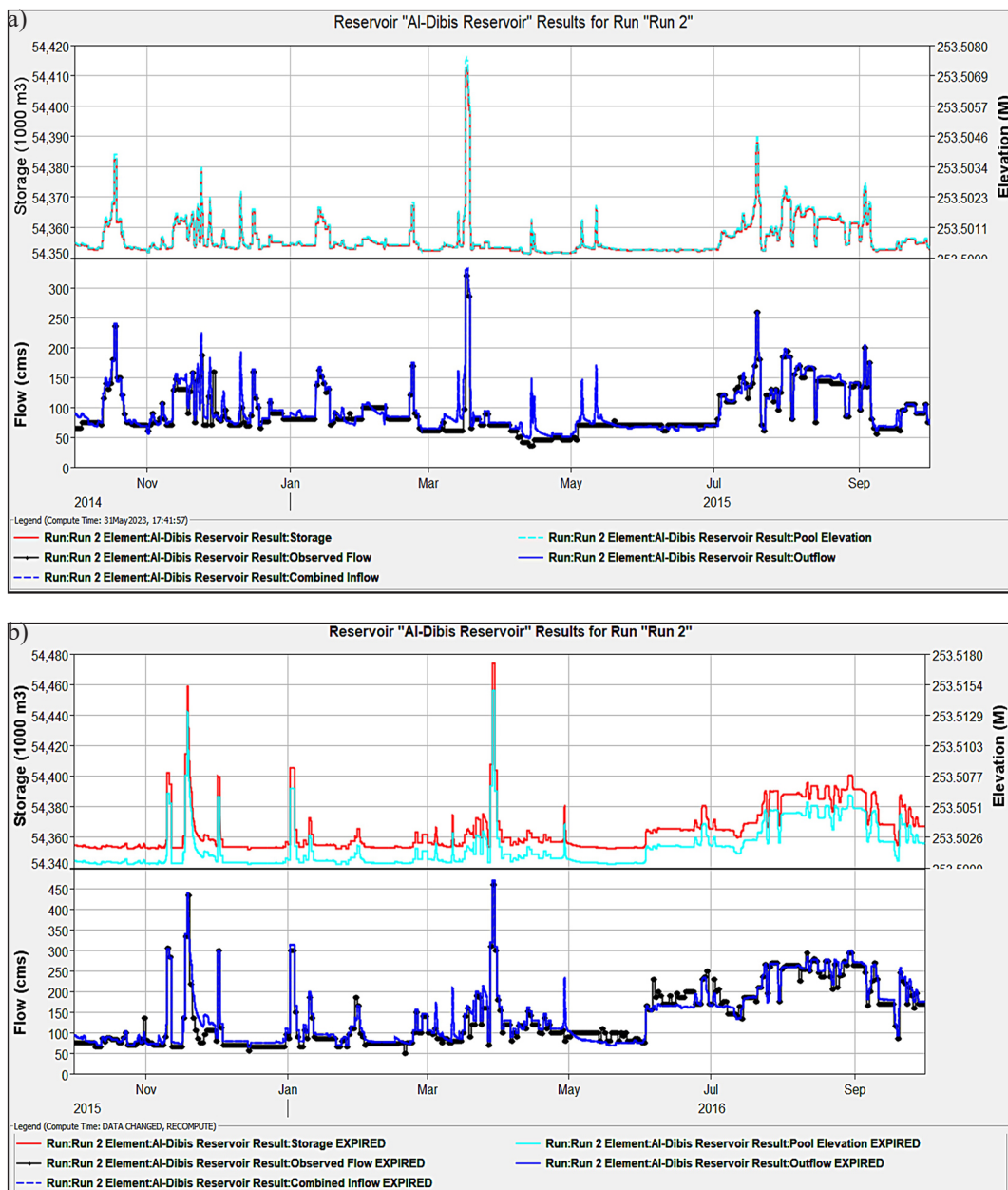


Figure 9. Calibrated hydrographs for the central region at Al-Dibis reservoir, (a) during 2014–2015, and (b) during 2015–2016

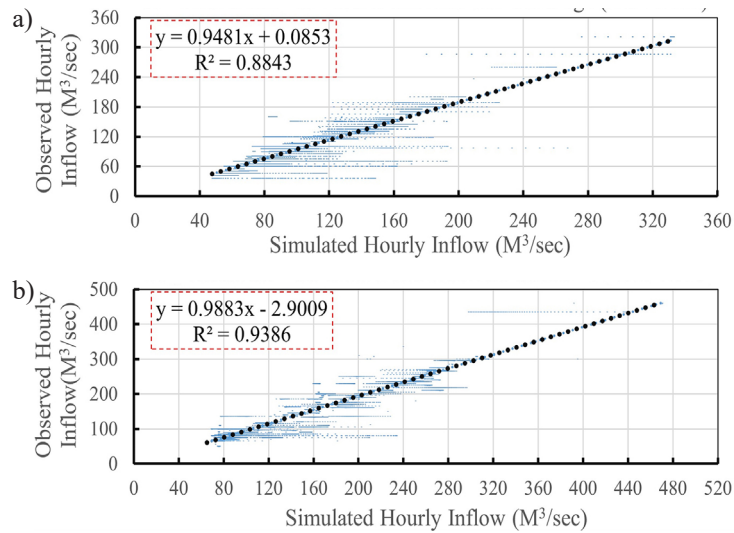


Figure 10. Regression analysis of Al-Dibis reservoir inflow discharge under the calibration phase, (a) for 2014–2015, and (b) for 2015–2016

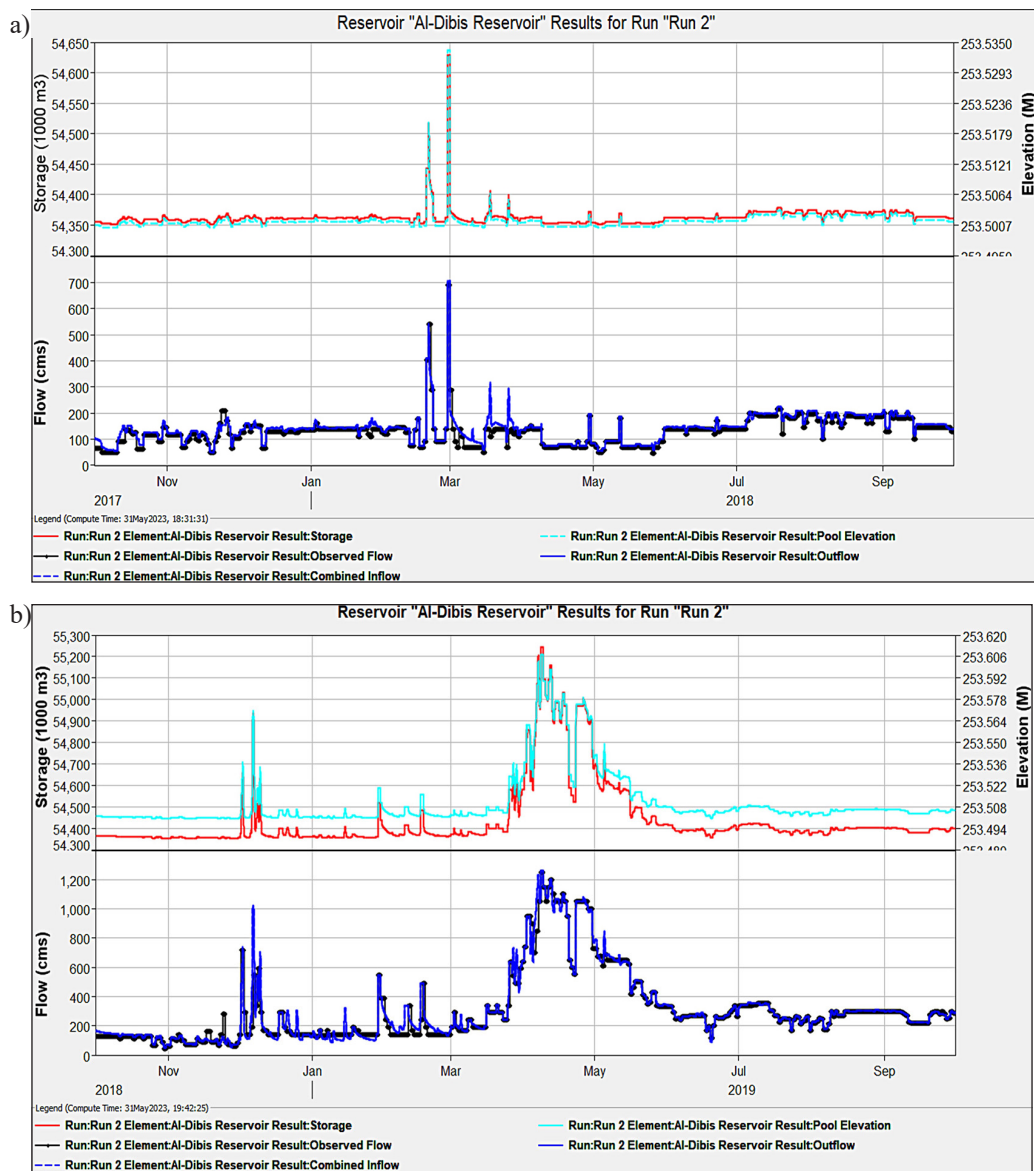


Figure 11. Validated hydrographs for the central region at Al-Dibis reservoir, (a) during 2017–2018, and (b) during 2018–2019

the limited contribution of the baseflow to the stream runoff in the central region of the LZR watershed.

The calibrated outlet hydrographs of the central region (at Al-Dibis Reservoir) are illustrated in Figure 9, the performance criteria are illustrated in Table 5, and the R^2 index is illustrated in Figure 10.

By comparing the resulting performance criteria under the calibration phase in Table 5 with those in Table 3, it is obvious that the model efficiency for the central region was very good.

Validation process

The validation process is used to check the suitability of the optimized parameters and the efficiency of the model through different periods, this

study was adopted the water years of 2017–2018 and 2018–2019 for the validation phase, See Figure 11. The performance criteria are illustrated in Table 6, and the R^2 index is illustrated in Figure 12.

By comparing the resulting performance criteria under the validation phase in Table 6 with those in Table 3, it is obvious that the model efficiency for the central region was very good.

Table 6. Performance criteria of the central region model under the validation phase

Water year	R^2	NSE	PBIAS %
2017–2018	0.901	0.872	7.58
2018–2019	0.949	0.948	2.31
Average	0.925	0.91	4.945

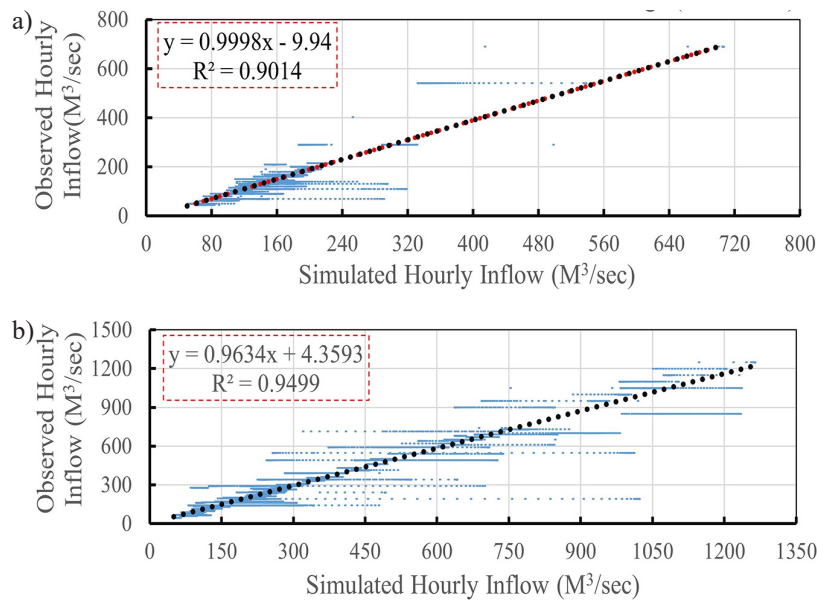


Figure 12. Regression analysis of Al-Dibis reservoir inflow discharge under the validation phase, (a) for 2017–2018, and (b) for 2018–2019

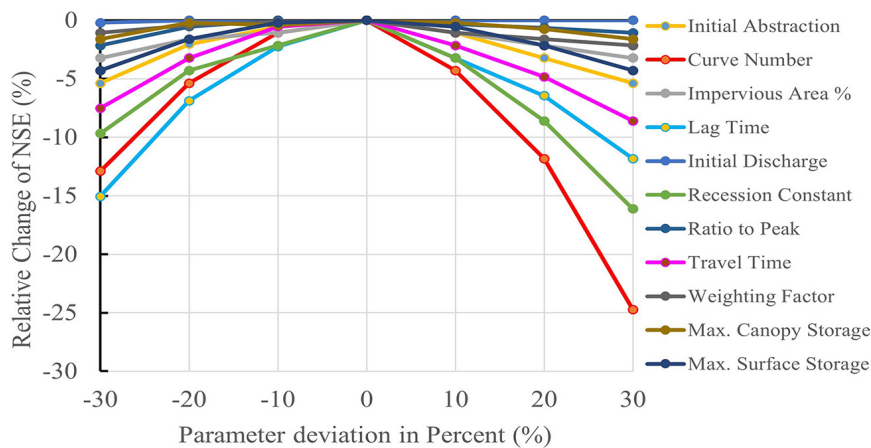


Figure 13. The percentage change of NSE statistic against the percentage deviation of each parameter for the sensitivity analysis process

Sensitivity analysis

The sensitivity analysis was achieved in this study to figure out the most influential parameters on the model efficiency by measuring the relative error percentage in the NSE value for each individual parameter deviation. In this study, all the parameters used in the sensitivity analysis are illustrated in Figure 13. It is very obvious that the model is very sensitive to the CN parameter, followed by the recession constant, lag time, travel time (K), and the initial abstraction (Ia) in descending order respectively, while the remaining parameters have only less than 5% change in the NSE value for each maximum deviation of any individual parameter. According to the previous, the sensitivity analysis indicates the importance of the accurate estimation of the CN parameter for the watershed hydrologic models generally, and the effectivity of this parameter in the LZR watershed model specifically.

DISCUSSION

In the LZR watershed, about 86% of the top soil was loamy soil with HSG type B, which has moderately low potential runoff, thus the lowest CN value was 56 (forest land). On the other hand, the major classes of vegetation cover in the LZR watershed, which were the shrubs/low shrubs lands and the crops lands, were the reasons for increasing the remaining values of the CN parameter reaching the highest value of the CN with 100 because of existing the water surface. The corrections of the CN parameter to the slope and initial abstraction effects were performed to enhance the CN values accuracy and the model efficiency, however, the initial and optimized values of the corrected CN parameter were close to each other as illustrated in Table 4, indicating the effectivity of these corrections on the CN parameter and the model efficiency. By observing the simulated and observed inflow hydrographs to Al-Dibis reservoir in Figs. 9 and 11 for the calibration and validation phases, it was noticed that the simulated inflow discharge hydrographs (in blue color) were just slightly larger than the observed hydrographs (in black color), this could be due to the neglecting of the water consumptions for the domestic usage, agricultural usage, and the usage for water treatment plants across the watershed. Moreover, for all the simulation runs illustrated in Figs. 9

and 11, the water elevation of Al-Dibis reservoir (in cyan color) was approximately constant with about 253.5 MASL with a small deviation, even though it was slightly increased at specific times, especially between March and May because of the high discharge flow that came from Dokan Dam where the snow starts to melt in the northern region, and because of the heavy rainfall in that period over the central region. According to the previous, it is obvious that Al-Dibis Dam's main role was just to control the outflow but not store any amount of water, therefore, the reservoir capacity of Al-Dibis Dam was kept approximately in the range of 54.35–54.65 MCM, except for the water year of 2018–2019 when it reached about 55.25 MCM due to the high incoming flow. In the end, the model was very good in general efficiency, since the performance indices of the model through the calibration and validation phases were very good as illustrated in Tables 5 and 6 in comparison with Table 3.

CONCLUSIONS

This study concluded the effectiveness of using the GIS environment, remote sensing (RS) data, and the HEC-HMS software for building a successful hydrologic model of any watershed in the world. The proposed hydrologic model of the LZR watershed in this study, specifically for the central region was very efficient due to the high values of the performance criteria achieved, since the R^2 , NSE, and PBIAS were 0.9115, 0.9, and 4.355% under the calibration phase, while 0.925, 0.91, and 4.945% values were achieved for the same criteria under the validation phase respectively, hence the validated model could be used effectively to estimate the runoff volume in any location between Dokan and Al-Dibis dams accurately. In addition, this study revealed that the correction of the CN parameter to the slope and initial abstraction resulted in very accurate values of the CN leading to an increase in the model accuracy and efficiency. Also, the baseflow component has a limited contribution to the stream runoff in the central region due to the low values of the initial baseflow discharge and the ratio-to-peak parameters of the Recession method. In the end, this study concluded the effectivity of the CN parameter since the CN was the most sensitive parameter in the hydrologic model of the LZR watershed.

REFERENCES

1. Ahbari A., Stour L., Agoumi A., Serhir N. 2018. Estimation of initial values of the HMS model parameters: Application to the basin of Bin El Ouidane (Azilal, Morocco). *Journal of Materials and Environmental Science*, 9(1), 305–317.
2. Al-Ansari N., Adamo N., Sissakian V.K., Knutsson S., and Laue J. 2018. Water Resources of the Tigris River Catchment. *Journal of Earth Sciences and Geotechnical Engineering*, 8(3), 21–42.
3. Al-Ansari N., Knutsson S. 2011. Toward prudent management of water resources in Iraq. *Journal of Advanced Science and Engineering Research*, 1(1), 53–67.
4. Alrammahi F.S., Hamdan A.N.A. 2022. Simulation of rainfall-runoff in the Diyala River Basin in Iraq using hydrological model by HMS with remote sensing, Geo-HMS and ArcGIS. *IOP Conference Series: Earth and Environmental Science*, 1120(1), 1-18.
5. Cronshey R. 1986. *Urban Hydrology for Small Watersheds-Technical Release 55 (TR55)*. United States Department of Agriculture (USDA)-Soil Conservation Service (SCS)-Engineering Division, USA.
6. Dinka M.O., Klik A. 2020. Temporal and spatial dynamics of surface run-off from Lake Basaka catchment (Ethiopia) using SCS-CN model coupled with remote sensing and GIS. *Lakes & Reservoirs: Research & Management*, 25(2), 167–182.
7. Environmental Systems Research Institute (ESRI), Land Use/ Land Cover (LULC) Layer, Available online: <https://www.arcgis.com/LULC>, (accessed on 10 March 2023).
8. Food and Agricultural Organization (FAO), FAO Soils Portal, Harmonized World Soil Database V 1.2, Available online: <https://www.fao.org/soils-portal/HWSD>, (accessed on 5 March 2023).
9. Gurmua A.T., Tolessa G.A. 2014. Surface Water Modeling Using SCS-CN Model-Hydroinformatic Approach. *European Academic Research*, 2(8), 10506–10522.
10. Halwatura D., Najim M. 2013. Application of the HEC-HMS model for runoff simulation in a tropical catchment. *Environmental Modelling & Software*, 46(8), 155–162.
11. Hamdan A.N.A., Almukhtar S., Scholz M. 2021. Rainfall-Runoff Modeling Using the HEC-HMS Model for the Al-Adhaim River Catchment, Northern Iraq. *Hydrology*, 8(2), 1–17.
12. Huang M., Gallichand J., Wang Z., Goulet M. 2006. A modification to the Soil Conservation Service curve number method for steep slopes in the Loess Plateau of China. *Hydrological Processes: An International Journal*, 20(3), 579–589.
13. Jabbar L.A., Khalil I.A., Sidek L.M. 2021. HEC-HMS Hydrological modelling for runoff estimation in Cameron Highlands, Malaysia. *International Journal of Civil Engineering and Technology*, 12(9), 40–51.
14. Kaffas K., Hrissanthou V. 2014. Application of a Continuous Rainfall-Runoff Model to the Basin of Kosynthos River Using the Hydrologic Software HEC-HMS. *Global NEST Journal*, 16(1), 188–203.
15. Khzr B.O., Ibrahim G.R.F., Hamid A.A., Ail S.A. 2022. Runoff estimation using SCS-CN and GIS techniques in the Sulaymaniyah sub-basin of the Kurdistan region of Iraq. *Environment, Development and Sustainability*, 24(2), 2640–2655.
16. Klari Z.M., Ibrahim S.A. 2021. Application of SCS-Curve Number Method to estimate Runoff using GIS for Gali-Bandawa Watershed. *Academic Journal of Nawroz University (AJNU)*, 10(1), 318–325.
17. National Aeronautics and Space Administration (NASA) Earth Data, Alaska Satellite Facility, ALOS PALSAR Satellite Dataset. Available online: <https://search.asf.alaska.edu>, (accessed on 20 Feb. 2023).
18. Noori A.M., Pradhan B., Ajaj Q.M. 2019. Dam site suitability assessment at the Greater Zab River in northern Iraq using remote sensing data and GIS. *Journal of Hydrology*, 574(1), 964–979.
19. Oleyiblo J.O., Li Z.J. 2010. Application of HEC-HMS for flood forecasting in Misai and Wan'an catchments in China. *Water Science and Engineering*, 3(1), 14–22.
20. Ouédraogo W.A.A., Raude J.M., Gathenya J.M. 2018. Continuous modelling of the Mkurumudzi River catchment in Kenya using the HEC-HMS conceptual model: Calibration, validation, model performance evaluation and sensitivity analysis. *Hydrology*, 5(3), 1–18.
21. Pokhrel K., Karki K.R. 2021. Rainfall-Runoff Simulation of Tamor River Basin using SCS-CN based HEC-HMS Model. In *Proceedings of 9th IOE Graduate Conference, Nepal*, 9(1), 129–139.
22. POWER. Data Access Viewer. Available online: <https://power.larc.nasa.gov> (accessed on 15 March 2023).
23. Saeedrashad Y., Guven A. 2013. Estimation of Geomorphological Parameters of Lower Zab River-Basin by Using GIS-Based Remotely Sensed Image. *Water Resources Management*, 27(1), 209–219.
24. Salman Q.M.K., Hamdan A.N.A. 2022. Estimation of the curve number for the Lesser Zab watershed using GIS and HEC-GeoHMS. In: *4th International Conference on Civil and Environmental Engineering Technologies (ICCEET)*, Kufa University, Iraq, 1-12.
25. Subramanya K. 2008. *Engineering Hydrology*. Tata McGraw-Hill Publishing Company Limited, India, 3rd Edition.
26. Tassew B.G., Belete M.A., Miegel K. 2019. Application of HEC-HMS model for flow simulation in the Lake Tana basin: The case of Gilgel Abay catchment, upper Blue Nile Basin, Ethiopia. *Hydrology*, 6(1), 1-17.
27. UN-ESCWA (United Nations Economic and Social Commission for Western Asia), and Federal Institute for Geosciences and Natural Resources, 2013. *Inventory of shared water resources in Western Asia*, Beirut, Lebanon.